

# Lanosterol Biosynthesis: The Critical Role of the Methyl-29 Group of 2,3-Oxidosqualene for the Correct Folding of this Substrate and for the Construction of the Five-Membered D Ring

Tsutomu Hoshino,\* Akifumi Chiba, and Naomi Abe<sup>[a]</sup>

**Abstract:** Lanosterol synthase catalyzes the polycyclization reaction of (3*S*)-2,3-oxidosqualene (**1**) into tetracyclic lanosterol **2** by folding **1** in a chair-boat-chair-chair conformation. 27-Nor- and 29-noroxidosqualenes (**7** and **8**, respectively) were incubated with this enzyme to investigate the role of the methyl groups on **1** for the polycyclization cascade. Compound **7** afforded two enzymatic products, namely, 30-norlanosterol (**12**) and 26-normalabariatriene (**13**; **12/13** 9:1), which were produced through the normal chair-boat-chair-chair conformation and an

atypical chair-chair-boat conformation, respectively. Compound **8** gave two products **14** and **15** (**14/15** 4:5), which were generated by the normal and the unusual polycyclization pathways through a chair-chair-boat-chair conformation, respectively. It is remarkable that the twist-boat structure for the B-ring formation was changed to an energetically favored chair structure for the

generation of **15**. Surprisingly, **14** and **15** consisted of a novel 6,6,6,6-fused tetracyclic ring system, thus differing from the 6,6,6,5-fused lanosterol skeleton. Together with previous results, we conclude that the methyl-29 group is critical to the correct folding of **1**, with lesser contributions from the other branched methyl groups, such as methyl-26, -27, and -28. Furthermore, we demonstrate that the methyl-29 group has a crucial role in the formation of the five-membered D ring of the lanosterol scaffold.

**Keywords:** alkenes • cyclization • enzyme catalysis • polycycles • terpenoids

## Introduction

Oxidosqualene cyclases convert (3*S*)-2,3-oxidosqualene (**1**) into nearly 120 different cyclic triterpene skeletons.<sup>[1]</sup> These enzymes impose either the chair or boat conformation on acyclic compound **1**, and the ensuing proton attack on the epoxide ring triggers the ring-forming reactions (C–C bond formation) with the correct regio- and stereochemical specificities, thus usually leading to the production of tetra- and pentacyclic scaffolds. Triterpene cyclases generate many chiral centers during the polyolefin cyclization cascade, and the mechanism for the cyclization/rearrangement reactions has attracted considerable attention.<sup>[1]</sup> The mechanism for the cyclization pathway was first proposed over a half-century ago by Eschenmoser et al. in 1955,<sup>[2]</sup> who with Cornforth<sup>[3]</sup> proposed that the chair-boat-chair-boat conformation for lanosterol biosynthesis affords protosterol cation **4** with a 17 $\alpha$ -oriented side chain (Scheme 1b). Later, Corey and

Virgil<sup>[4]</sup> proposed the 17 $\beta$ -oriented side chain **3** as the true protosterol cation intermediate based on the analysis of the stereochemistry of the enzymatic products of 20-oxa-2,3-oxidosqualene<sup>[4]</sup> and (20*E*)-20,21-dehydro-2,3-oxidosqualene<sup>[5]</sup> by hog-liver lanosterol synthase. Furthermore, through the subsequent backbone-rearrangement process, **3** can be converted into **2** with a 20*R* configuration through a least-motion pathway that involves only a small rotation (<60°) about the C-17–C-20 axis, but a large rotation (120°) is required prior to proton migration from C-17 to C-20 to generate the *R* configuration, as observed in **4**.<sup>[4]</sup> Thus, a chair-boat-chair-chair conformation (Scheme 1a) that leads to the protosterol cation **3** is now accepted as an intermediate in lanosterol biosynthesis.<sup>[6,7]</sup>

Numerous studies on lanosterol synthase-mediated reactions of substrate analogues of **1** have been reported.<sup>[1–8]</sup> Corey et al. and van Tamelen et al. reported the enzymatic products of 26-noroxidosqualene,<sup>[9]</sup> 28-noroxidosqualene (**5**),<sup>[10]</sup> and 27,28-bisnoroxidosqualenes (**6**; Figure 1).<sup>[11]</sup> Analogues of 26-noroxidosqualene and **5** were converted into 19-nor- and 18-norlanosterols **10**,<sup>[9,10]</sup> respectively, thus indicating that the normal chair-boat-chair-chair conformation was imposed by lanosterol synthase. The tetracyclic product **11**, which consists of the ring system of both a 6,6,5-fused tricycle and an isolated four-membered ring, was created from **6**, thus indicating that **6** was folded in an abnormal chair-chair-boat conformation.<sup>[11]</sup> Interestingly, the conformation of the B ring was converted from a twist boat into a chair structure. Accordingly, Corey et al. proposed that the

[a] Prof. Dr. T. Hoshino, A. Chiba, N. Abe  
Department of Applied Biological Chemistry  
Faculty of Agriculture  
and Graduate School of Science and Technology  
Niigata University, Ikarashi 2-8050  
Nishi-ku, Niigata, 950-2181 (Japan)  
Fax: (+81)25-262-6854  
E-mail: hoshitsu@agr.niigata-u.ac.jp

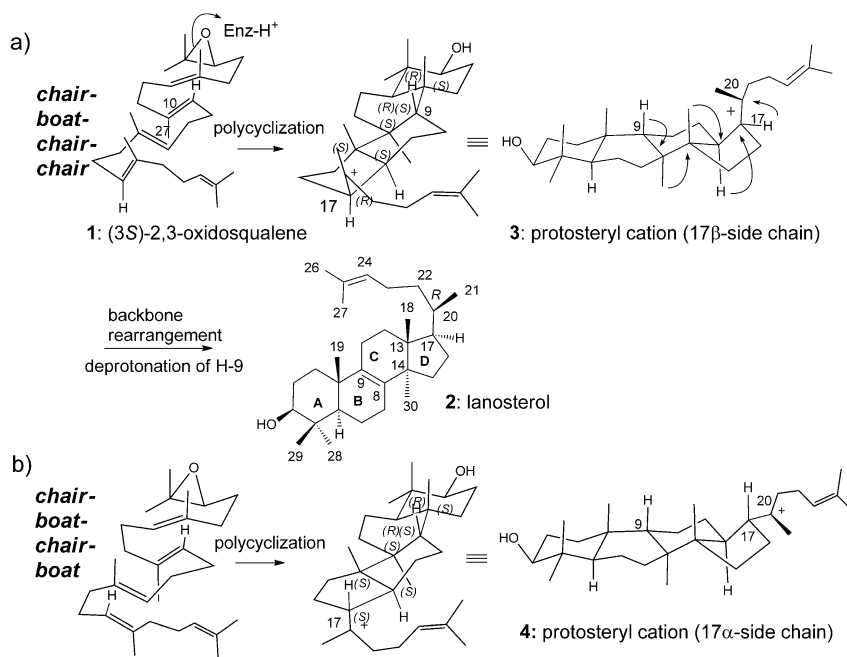
Supporting information for this article is available on the WWW under <http://dx.doi.org/10.1002/chem.201201779>.

methyl-27 group at C10 of **1** was critical for the correct folding in the polycyclization and rearrangement reaction.<sup>[11]</sup> Clayton et al.<sup>[12]</sup> and Corey et al.<sup>[13]</sup> examined the cyclization

reaction of 1-nor and 25-nor analogues and reported that the 1-nor analogue underwent the polycyclization reaction to yield 29-norlanosterol, whereas the 25-nor analogue under-

went no reaction. However, no report has appeared concerning the enzymatic reactions of **7** and **8**, in which the methyl groups present in **1** at C-10 and C-19, respectively, are absent.

Herein, we describe the enzymatic products of **7** and **8** and discuss how the branched methyl groups present in **1** influence the conformation during the polycyclization cascade. We report that the methyl-29 group at C-19 is more important to the correct folding of **1**, especially with regard to the boat structure of the B ring relative to the methyl-27 group at C-10. We also describe the unprecedented cyclization pathway that generates a novel skeleton that consists of a 6,6,6,6-fused tetracyclic ring system, which differs from the 6,6,6,5-fused lanosterol skeleton.



Scheme 1. Folding conformation of (3S)-2,3-oxidosqualene **1** for lanosterol biosynthesis.

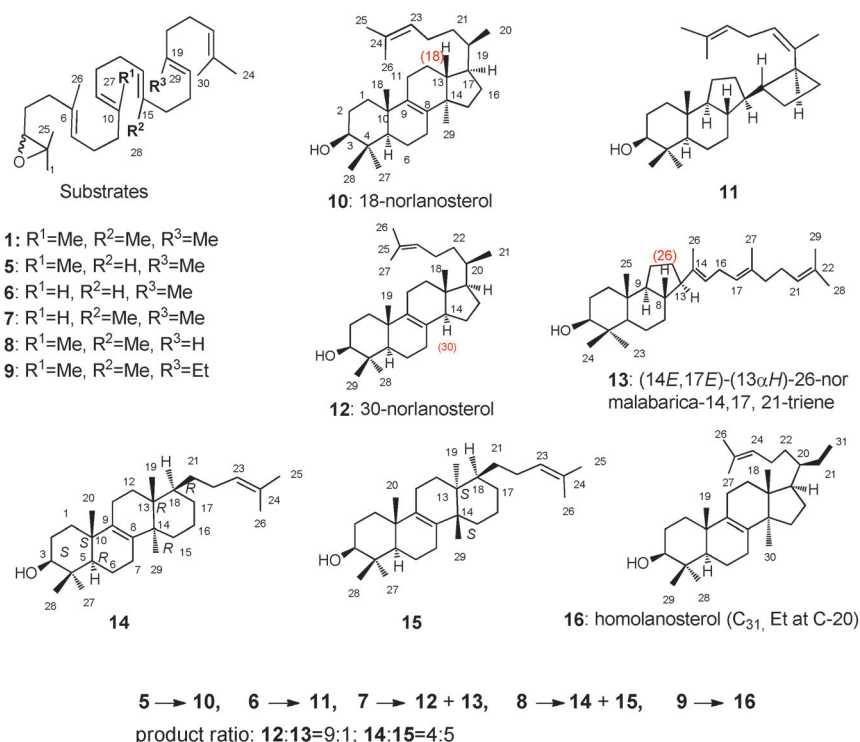
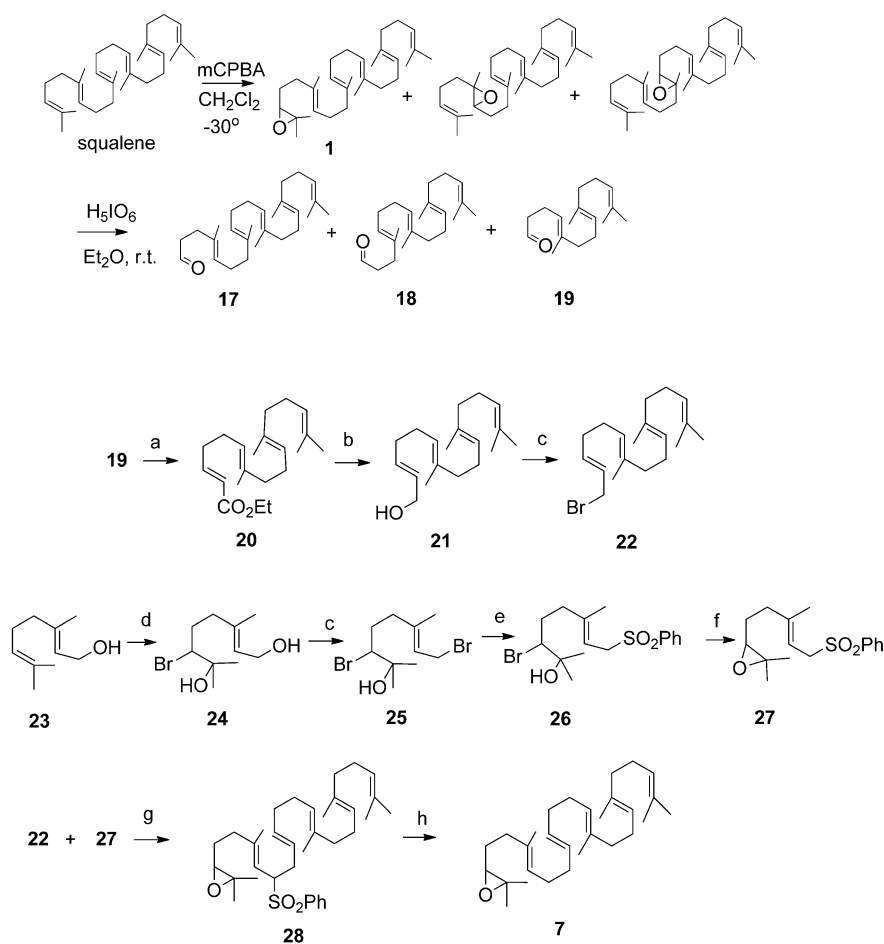


Figure 1. Structures of substrate analogues **5–9** and the enzymatic products **10–16**. The fundamental core of **13** is the same as that of malabaricatriene triterpene, but **13** lacks the Me-26 group of the malabaricatriene skeleton that is situated at C-8. The black numbering of the carbon atoms is used for the assignments of the NMR spectroscopic data and is arbitrary. The red numbering for **10**, **12**, and **13** is based on the numbering of the parent skeletons (lanosterol and malabaricatriene with C<sub>30</sub>).

## Results

**Syntheses of noroxidosqualenes 5, 7, and 8:** The synthesis of **7** was performed according to Scheme 2. (4E,8E)-5,9,13-Triethyltetradeca-4,8,12-trienal (**19**), prepared from squalene by treating with MCPBA and periodic acid, was subjected to the Wittig–Horner reaction with ethyl diethylphosphonoacetate to yield (2E,6E,10E)-ethyl-7,11,15-trimethylhexadeca-2,6,10,14-tetraenoate (**20**; 87%). Ethyl ester **20** was converted into the corresponding alcohol **21** by reduction with diisobutylaluminum hydride (DIBAL-H; 93%), which was then transformed into bromide **22** by using PBr<sub>3</sub>. Commercially available geraniol **23** was treated with NBS to give bromohydrin **24** (53%), followed by bromination with PBr<sub>3</sub> to afford



Scheme 2. Synthetic scheme of 10-noroxidosqualene (**7**). 1)  $(\text{Et}_2\text{O})_2\text{POCH}_2\text{CO}_2\text{Et}$ , NaH,  $\text{Et}_2\text{O}$ , THF,  $-40^\circ\text{C}$ ; 2)  $(i\text{-C}_4\text{H}_9)_2\text{AlH}$ ,  $\text{Et}_2\text{O}$ ,  $-40^\circ\text{C}$ ; 3)  $\text{PBr}_3$ , THF,  $0^\circ\text{C}$ ; 4) NBS, THF,  $0^\circ\text{C}$ ; 5)  $\text{PhSO}_2\text{Na}\cdot 2\text{H}_2\text{O}$ , DMF,  $0^\circ\text{C}$ ; 6)  $\text{K}_2\text{CO}_3$ , MeOH, room temperature; 7)  $n\text{BuLi}$ , THF/HMPTA (4:1),  $-78^\circ\text{C}$ ; 8)  $\text{LiBEt}_3\text{H}$ ,  $\text{Et}_2\text{O}$ ,  $0^\circ\text{C}$ . HMPTA = hexamethylphosphorotriamide, MCPBA = *meta*-chloroperbenzoic acid, NBS = *N*-bromosuccinimide.

**25**. Bromide **25** was treated with sodium benzenesulphonate to yield the phenylsulfone derivative **26**, which was converted into epoxide **27** (61%). The coupling reaction of **27** and **22** was carried out in THF containing HMPTA by adding  $n\text{BuLi}$ , thus yielding the phenylsulfone derivative **28** of oxidosqualene (13%). The removal of the phenylsulfonyl group was carried out with the super hydride reagent to obtain the desired **7** (76%).

The syntheses of noranalogues **5** and **8** were performed by using essentially identical methods to that for **7** with the same reagents. Compounds **21** and **18** were used for the preparation of **5** and **8**, respectively (the experimental details are described in the Supporting Information). The ethyl-substituted analogue **9** was prepared according to the method described in the Supporting Information.

**The structures of products 12–15 from noroxidosqualenes 7 and 8 and the cyclization pathways:** Products **12** and **13** were generated by incubating ( $\pm$ )-**7** with hog-liver lanosterol synthase and were purified by column chromatography and

HPLC. Compound **12** was separated as a pure compound, and **13** was acetylated before purification. The  $^1\text{H}$  and  $^{13}\text{C}$  NMR (600 and 150 MHz, respectively) spectra of **12** measured in  $\text{CDCl}_3$  revealed one olefinic proton ( $\delta_{\text{H}}=5.09$  ppm, t,  $J=6.9$  Hz), two vinylic methyl groups ( $\delta_{\text{H}}=1.68$  and  $1.60$  ppm, each 3H, s), and one tetrasubstituted double bond (C-8:  $\delta_{\text{C}}=128.0$  ppm, s; C-9:  $\delta_{\text{C}}=135.9$  ppm, s). Heteronuclear multiple-bond correlations (HMBC) were observed for Me-19/C-9, H-14/C-8, and H-14/C-9. No NOE interactions for H-14/Me-18 and clear NOE interactions for H-14/H-7/H-17 established the structure of the lanosterol skeleton for **12** (see Figure S5 in the Supporting Information), which was ascertained to be 30-norlanosterol with  $20R$  stereochemistry produced through the normal cyclization pathway (Scheme 1a). Compound **12** is one of the intermediates in cholesterol biosynthesis and is known as a testicular meiosis-activating sterol.<sup>[14]</sup> The acetate of product **13** had three olefinic protons and four vinylic methyl groups, thus suggesting a tricyclic compound, which was further veri-

fied by detailed HMBC analysis (see Figure 2a and the Supporting Information). Definitive NOE interactions for H-9/H-13 and Me-25/H-8 demonstrated that the structure of **13** is as shown in Figure 2, thus allowing **7** to adopt a chair-chair-boat conformation (Scheme 3a). The cationic intermediate **29** thus formed could be quenched by the deprotonation of H-15 to give the *E* geometry, which was confirmed by the clear NOE interaction of Me-26/H-16 (see the Supporting Information). This conformation is consistent with that proposed for the polycyclization reaction of 27,28-bisnoroxidosqualene **6**.<sup>[11]</sup> However, it should be noted that the ratio of fully cyclized **12**/partially cyclized **13** was determined to be 9:1 by GC analysis, thus suggesting that the influence of the small hydrogen substitution at C-10 on the polycyclization cascade is not significant.

Products **14** and **15** were generated by incubating ( $\pm$ )-**8** with hog-liver lanosterol synthase and their acetates were purified with reversed-phase HPLC.  $^1\text{H}$  NMR (see the Supporting Information) and DEPT analysis revealed that both products had one olefinic proton ( $\delta_{\text{H}}=5.10$  ppm, t,  $J=$

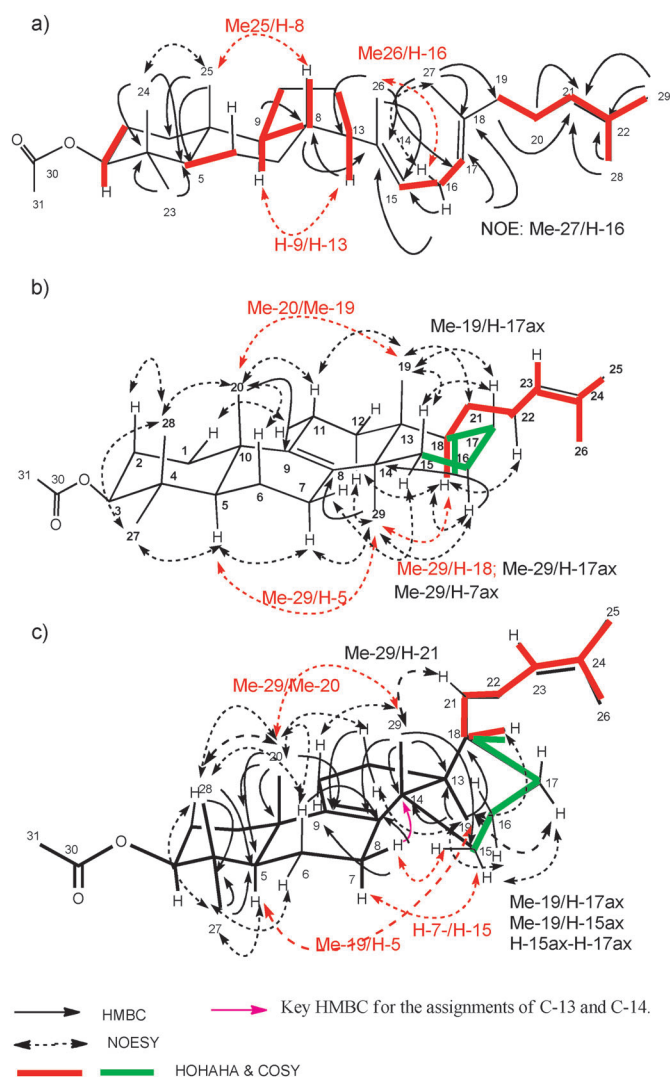


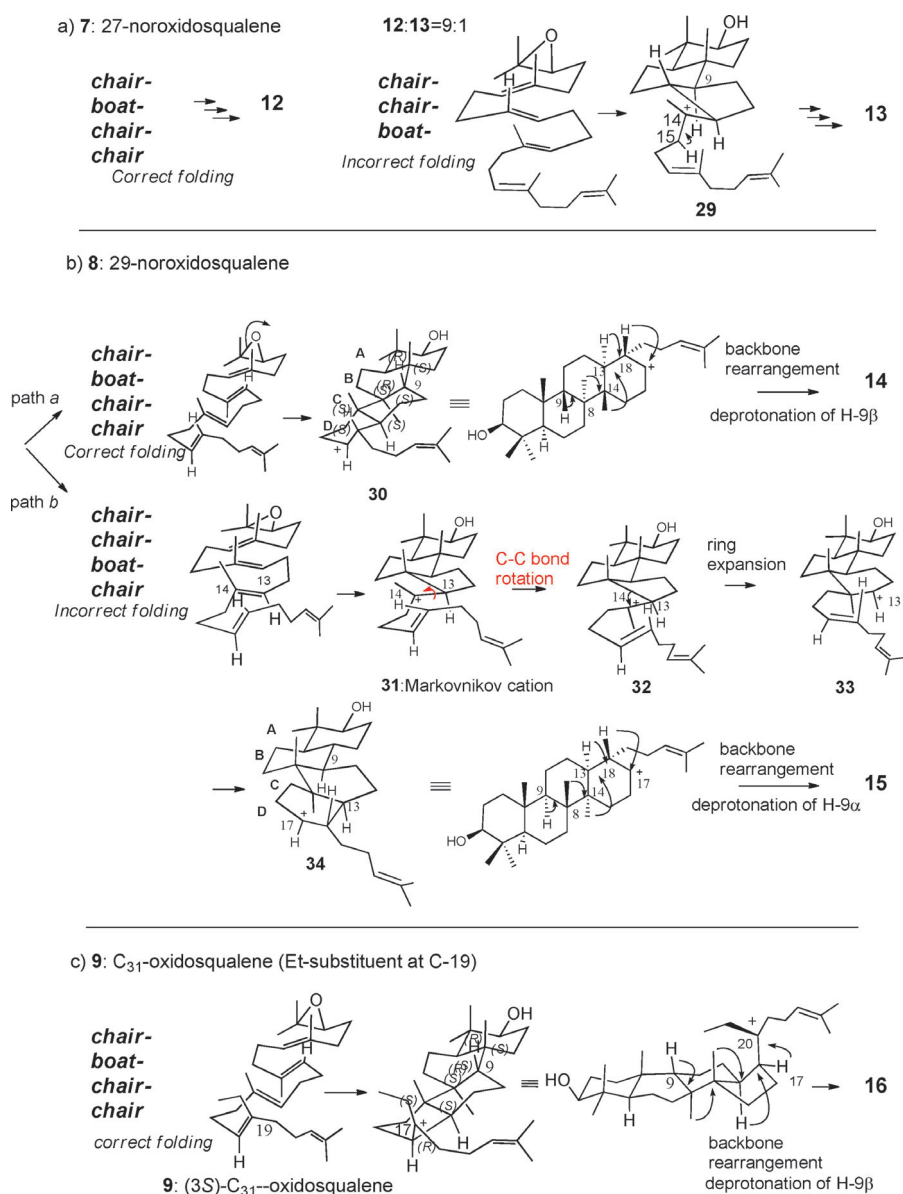
Figure 2. Key data of COSY, HOHAHA, NOE, and HMBC spectra for proposing the structures of products a) **13**, b) **14**, and c) **15**, which were measured in  $\text{CDCl}_3$ ,  $\text{C}_6\text{D}_6$ , and  $[\text{D}_6]\text{acetone}$  (see the Supporting Information).

7.0 Hz) and one tetrasubstituted double bond ( $\delta_{\text{C}}=136$  ppm, s;  $\delta_{\text{C}}=134$  ppm, s), as seen in lanosterol structure **2**. In the HOHAHA spectra of the acetates of **14** and **15** (see the Supporting Information), the olefinic proton H-23 of both products had correlations with Me-25, Me-26, H-22, H-21, and H-18. The Me-19 group had a HMBC cross-peak for C-18 ( $\delta_{\text{C}}=40.43$  ppm, d for **14**-acetate;  $\delta_{\text{C}}=45.24$  ppm, d for **15**-acetate). The following COSY and HOHAHA networks were found from H-18: H-17, H-16, and H-15, and a definitive HMBC correlation of Me-29/C-15 was found. These data clearly demonstrated that both **14** and **15** consisted of a six-membered cycle for the D ring, but not a five-membered ring. The mass spectra (EI) of both the acetate salts of **14** and **15** were identical to each other (see the Supporting Information), thus suggesting that the structure of **14** differed from that of **15** only with regard to stereochemistry. It is to

be noted that the Me-19 and Me-29 groups must be placed in a *trans* arrangement because both **14** and **15** had no NOE interaction between the Me-19 and Me-29 groups, as seen in lanosterol.

The stereochemistry of **14** and **15** was carefully inferred on the basis of detailed analysis of the NOESY spectra. Some of the angular methyl proton signals overlapped or were contiguously located. The NMR spectra of the acetate salts of **14** and **15** were measured in different solvents such as  $\text{CDCl}_3$ ,  $\text{C}_6\text{D}_6$ , and  $(\text{CD}_3)_2\text{CO}$  to separate these signals (see the Supporting Information). The NOE interactions of authentic lanosterol acetate were also collected in the different solvents (see the Supporting Information) and used as a reference to determine the stereochemistry of **14** and **15**. In the NOESY spectra of the **14**-acetate (see the Supporting Information), definitive cross peaks of Me-29/H-5 $\alpha$  and Me-19/Me-20 $\beta$  confirmed the configurations of the Me-29 $\alpha$  and Me-19 $\beta$  groups. Furthermore, a strong NOE interaction between Me-29 and H-18 was observed for **14**, but no NOE interaction for Me-19/H-18 indicated that both Me-29 $\alpha$  and H-18 $\alpha$  are arranged in an axial disposition in the chair structure. A clear NOE interaction for Me-19 $\beta$ /H-21 was observed, which is indicative of Me-19 $\beta$  and H-21 $\beta$  (Figure 2b). Thus, the following stereochemistry was assigned for **14**: 3*S*, 5*R*, 10*S*, 13*R*, 14*R*, 18*R*. On the other hand, clear NOE interactions for Me-19/H-5 $\alpha$  and Me-20 $\beta$ /Me-29 were found for the **15**-acetate, but no NOE interaction for Me-29/H-5 $\alpha$  (see the Supporting Information), unambiguously indicated the stereochemistry of Me-29 $\beta$  and Me-19 $\alpha$ . Definitive NOE interactions for Me-29 $\beta$ /H-21 and Me-19 $\alpha$ /H-18 indicated that H-21 and H-18 were oriented in axial and equatorial dispositions, respectively (Figure 2c). The chair structure of the D ring was further supported by strong NOE interactions for Me-19/H-17 $\text{ax}$ , Me-19/H-15 $\text{ax}$ , and H-15 $\text{ax}$ /H-17 $\text{ax}$ . Thus, the stereochemistry of **15** was determined as follows: 3*S*, 5*R*, 10*S*, 13*S*, 14*S*, 18*R*. It is noticeable that the configurations at C-13 and C-14 of **14** are the same as those of **2**, but those of **15** are opposite to those of **2**. Molecular modeling of the acetate salts of **14** and **15** supported the configurations at C-13 and C-14 (see the Supporting Information). A comparison of the proton chemical shifts of the angular Me groups of the acetate salts of **14** and **15** with those of lanosterol acetate (see the Supporting Information) further supported the configurations. Thus, the structures of **14** and **15** are depicted as shown in Figure 1.

It is possible that 29-noroxidosqualene (**8**) adopts a chair-boat-chair-chair conformation (path a in Scheme 3b) to afford cation intermediate **30**, which could then undergo 1,2-hydride and methyl shifts in an antiperiplanar fashion followed by the deprotonation of H-9 to yield **14**. A chair-chair-boat-chair conformation could be adopted for the formation of **15** (path b in Scheme 3b) to give the 6,6,5-fused tricyclic cation **31** with H-13 $\alpha$ . The C-13–C-14 bond axis could rotate to afford cation **32** with an  $\alpha$ -oriented Me group at C-14, and the subsequent ring expansion could give the 6,6,6-fused tricyclic cation **33**, followed by further cyclization to produce the 6,6,6,6-fused tetracycle **34**. The subse-

Scheme 3. Folding conformations of substrate analogues **7–9**, thus leading to products **13–16**.

quent backbone rearrangements and the proton elimination of H-9 could result in the production of **15**.

Other folding conformations of **8** were envisaged and the corresponding cyclization products were evaluated to validate the proposed structures of **14** and **15** (see the Supporting Information, pages S50–S53). To acquire the configuration of Me-29 $\alpha$  for **15**, which is identical to that of **2**, the conformation for B-ring construction must be a boat form. Three other possible folding conformations that lead to products **56–58** are assumed, but the NOE interactions of the **15**-acetate are inconsistent with the proposed structures of **56–58** (see the Supporting Information, page S50).

In contrast, the chair-folding in the B-ring formation results in a  $\beta$ -oriented Me-29 group. All of the possible folding conformations are listed in the Supporting Information (page S51). Examples 1–4, in which no bond rotation and no

ring expansion occur, would lead to **59–62**, but these structures do not agree with the NOE data of **15**-acetate. The reaction schemes of example 5 (see the Supporting Information, page S51) and path b in Scheme 3 are accompanied by a C-13–C-14 bond rotation on Markovnikov cation intermediates prior to the ring expansion (5 $\rightarrow$ 6-membered ring), then further cyclization and backbone rearrangements lead to product **15** (**63** is identical to **15**) that fully coincides with the observed NOE data. Thus, the bond rotation prior to the ring expansion is required to fulfill the stereochemistry of **15**. A higher production of **15** than **14** (**15/14** 5:4) indicates that the Me-29 group is more crucial for the correct folding of **1** for the biosynthesis of **2** relative to Me-27 (**12/13** 9:1).

In our experiment, the incubation of **5** (see Figure S3 in the Supporting Information for the synthetic details) gave **10** as the sole enzymatic product (see Figure S10 and the NMR spectroscopic data in the Supporting Information, pages S54–S55), which was in good agreement with the results reported by van Tamelen et al.<sup>[10]</sup>

#### Time-dependent inactivation by noroxidosqualenes **5**, **7**, and **8**:

Compounds **12–15** were produced in very small amounts. We investigated the possibility that time-dependent inactivation occurred during the incubations of **7** and **8**. Kinetic analysis revealed the following parameters: IC<sub>50</sub> = 180  $\mu$ M,  $k_{\text{inact}}$  = 0.0037 min<sup>-1</sup>,  $K_I$  = 0.013  $\mu$ M for **7**; IC<sub>50</sub> = 76  $\mu$ M,  $k_{\text{inact}}$  = 0.0068 min<sup>-1</sup>,  $K_I$  = 0.015  $\mu$ M for **8** (see Figure S11 in the Supporting Information). It was reported that **6** displayed time-dependent irreversible inhibition.<sup>[11]</sup> Time-dependent inhibition was also observed for **5** in our experiment ( $k_{\text{inact}}$  = 0.0065 min<sup>-1</sup>,  $K_I$  = 0.020  $\mu$ M), although this finding has not been previously reported.<sup>[10]</sup>

**Cyclization pathway of the bulkier ethyl-substituted oxidosqualene 9:** Previously,<sup>[15–17]</sup> we reported the results of incubation experiments of analogues of **1** bearing an ethyl substituent at C-10 and/or C-15 with hog-liver cyclase (see Figure S12 in the Supporting Information). Analogue **64** substi-

tuted with an ethyl group at both C-10 and C-15 afforded only the monocyclic products **67** and **69**.<sup>[15]</sup> Analogue **65** with an ethyl substituent at C-10 gave monocycles **68** and **70**, tricycle **71**, and tetracycle **73** (**68/70/71/73** 1:1:1:1).<sup>[16]</sup> Analogue **66** with an ethyl group at C-15 yielded tricycle **72** and tetracycle **74** (**72/74** 1:2.6).<sup>[17]</sup> The polycyclization reaction of **64** afforded the monocyclic compounds **68** and **70** as the main products, but the reaction of **66** proceeded to the tri- and tetracyclic stages **72** and **74**, respectively. An ethyl group is slightly bulkier than a methyl group, thus leading us to conclude that the binding site that accommodates the methyl group of **1** is more discriminating than the binding site for the methyl group of C-15.<sup>[17]</sup>

Synthesized ( $\pm$ )-**9** (6 mg) was incubated with partially purified hog-liver cyclase to examine the effect of the bulkier substituent at C-19 on the polycyclization pathway. The enzymatic product was purified by column chromatography on SiO<sub>2</sub> gel and normal-phase HPLC (hexane/THF 100:0.5) to yield pure **16** (1.8 mg) as the sole enzymatic product. The <sup>1</sup>H and <sup>13</sup>C NMR spectra (in CDCl<sub>3</sub>) indicated the following functional groups: one olefinic proton ( $\delta_{\text{H}}=5.11$  ppm, t,  $J=6.8$  Hz), two vinylic methyl protons (Me-26:  $\delta_{\text{H}}=1.682$  ppm, s, 3H; Me-27:  $\delta_{\text{H}}=1.605$  ppm, s, 3H), and one tetrasubstituted double bond ( $\delta_{\text{C}}=134.4$  ppm, s;  $\delta_{\text{C}}=134.3$  ppm, s), thus indicating a lanosterol skeleton for **16**. The detailed analyses of the 2D NMR spectra were in good agreement with homolanosterol structure, in which ethyl group is substituted at C-20 (see Figure S13 in the Supporting Information for the NMR spectroscopic analyses). The 20R stereochemistry is credible in light of the cyclization pathway (Scheme 3c). High production of **16** indicates that the binding site that accepts C-19 is somewhat more loosely packed than the binding sites for C-10 or C-15 and can accept the bulky ethyl group, albeit with the somewhat lower affinity of **9** for this cyclase relative to that observed for **1** ( $K_{\text{m}}=231$   $\mu\text{M}$ ,  $V_{\text{max}}=0.47$   $\mu\text{M min}^{-1}$  for **9**;  $K_{\text{m}}=75$   $\mu\text{M}$ ,  $V_{\text{max}}=0.33$   $\mu\text{M min}^{-1}$  for **1**). Kinetic analysis showed that **9** did not undergo time-dependent inhibition. The polycyclization reaction of the bulkier ethyl-substituted **65** and **66** halted at the premature stage to afford mono- and tricyclic products (see Figure S12 in the Supporting Information). In the reaction of **9**, full polycyclization occurred without stopping at the intermediate stage. In contrast, the methyl-deficient 26-noroxidosqualene and 27-noroxidosqualene **7** (substituted with a less-bulky hydrogen atom) gave 19-norlanosterol<sup>[9]</sup> and 30-norlanosterol as the main products (ca. 90%; see Figure 1), respectively, which resulted from the complete polycyclization reaction that proceeded through the normal folding conformation. Therefore, these results strongly indicate that the binding site involved in the early steps of the polycyclization is tightly packed and more discriminating, whereas the binding site for the later step is less compact and can accept larger substituents.

## Discussion

X-ray crystallographic analysis of human lanosterol synthase was reported in 2004.<sup>[18]</sup> It revealed that the tyrosine (Tyr) residue Tyr98 is well positioned to enforce the energetically unfavorable boat folding for the B-ring formation of **3** by pushing the methyl group at C-10 of **1** below the molecular plane (Scheme 1a).<sup>[18]</sup> A less-bulky hydrogen atom in **7** is substituted at C-10. The increased space between the Tyr residue and the hydrogen atom at C-10 may have allowed freer motion of this substrate, thus leading to the adoption of the energetically favored chair structure in the B ring and the production of **13**. The altered chair folding for the B ring could further exert influence on the conformation for the subsequent C-ring formation; a chair form for the C ring in lanosterol biosynthesis could be changed into a boat structure (Scheme 3a).

Wu et al. reported that the F699N or F699M variants of *S. cerevisiae* lanosterol synthase produced the tricyclic compound (14*E*,17*E*)-(13 $\alpha$ H)-malabarica-14,17,21-triene,<sup>[19]</sup> the skeleton of which is the same as that of **13** (i.e., 26-normalabaricatriene). This report is the first that describes the successful alteration of the conformation of the B ring from boat to chair by using mutagenesis experiments. The phenylalanine (Phe) residue Phe699 is located near the D-ring-formation site<sup>[19]</sup> and is chemically equivalent to the Phe601 residue of squalene-hopene cyclase, which stabilizes the intermediate cation through cation- $\pi$  interactions.<sup>[1a,22,23]</sup> It was postulated that these mutations might cause inappropriate positioning of the side chain and partially disrupt the transient dipole interactions between the carbocationic intermediate and the hydroxy group of the Tyr99 (equivalent to Tyr98 of human lanosterol synthase) and/or Tyr707 residues, thus leading to the atypical chair-chair-boat conformation (as seen in **29**).<sup>[19]</sup> Furthermore, it was demonstrated that by varying the size of the side chain through a single amino acid substitution at the residues of Tyr99-Tyr707-Ile705-Phe699, which are highly conserved (see Figure S14 in the Supporting Information) and are in proximity to the B-, C-, and D-ring-formation sites, the substrate conformation and polycyclization cascade are altered.<sup>[19-21]</sup> Thus, the appropriate sizes of the active-site residues to allow for steric bulk are crucial to determine the substrate folding. In turn, the steric size at the methyl-substituted positions on substrate **1** also influenced the conformation and/or the polycyclization cascade (e.g., truncation of the annulation reaction), as demonstrated by the incubation experiments of **7**, **8**, and ethyl-substituted analogues **9** and **64-66** with the native lanosterol cyclase from hog-liver. Therefore, it is apparent that the steric-size match between the substrate and the catalytic site is critical to the correct folding of **1** and the cyclization pathway.

Analogue **8** could undergo two different cyclization pathways. Product **14** could be produced under a normal polycyclization pathway (through a chair-boat-chair-chair conformation). However, it is difficult to discern why **8** was folded in a chair-chair-boat-chair during the polycyclization cascade

to afford **15** (path b in Scheme 3). Notably, the conformation of the B ring is changed from the boat to chair form. As described above, the recognition site of the Me-29 group of **1** is less compact than necessary because the bulkier ethyl-substituted **9** was also accepted as the substrate and folded in the normal conformation (Scheme 3c) to afford homolanosterol **16**. Binding between the less-bulky hydrogen atom at C-19 and the loosely packed binding site may have given rise to excess space and free motion at the B-ring-formation site, thus allowing the thermodynamically favored chair structure to be formed instead of the constrained boat conformation. Furthermore, the improper arrangement of **8** inside the reaction cavity could further contribute to the misfolded boat form at the C-ring-formation site, as mentioned in the production of **13**. The increase in the cleft volume at the D-ring-formation site, which could be generated by the lack of the Me-29 group, could further allow the C-13–C-14 bond rotation in the Markovnikov cation **31** prior to the ring expansion, although this rotational movement is usually unlikely when the substrate is tightly constricted by the enzyme active sites.

Why was the six-membered D ring constructed for **14** and **15** instead of the five-membered D ring? The intermediary cation **33** cannot generate a stable tertiary cation such as **3** in the subsequent annulation reaction, but affords only a secondary cation irrespective of the formation of five- or six-membered D rings. Therefore, a six-membered ring with less steric strain than a five-membered ring could be constructed for both products **14** and **15**. The H-9 $\beta$  atom of intermediate **30** was eliminated for the formation of **14** (path a in Scheme 3), as seen in the biosynthesis of **2**, but H-9 $\alpha$  of intermediate **34** was abstracted for that of **15** (path b in Scheme 3). At the present time, the reason remains uncertain why the stereochemically different H-9 could be eliminated. One possible explanation is that the basic (polar) residue responsible for the deprotonation reaction of H-9 $\alpha$  may be different from that for H-9 $\beta$ . The X-ray crystal structure of human lanosterol synthase has revealed that the phenolic Tyr503 residue that is hydrogen bonded to the histidine (His) residue His232 and situated above the molecular plain of **3** is involved in the deprotonation reaction of H-9 $\beta$ .<sup>[17]</sup> The H-9 $\beta$  atom of **30** could be eliminated in the same mechanism as that of **3** to form **14**. Another polar residue that is located below the molecular plain of **34** may have abstracted H-9 $\alpha$  to yield **15**. For the production of **13** and **11**, the different other polar residues would have worked for the deprotonation reaction.

Further studies, including X-ray crystallography studies of the complex between 29-nor-2,3-iminosqualene (a potent inhibitor) and lanosterol cyclase are required to validate our assumptions or to understand precisely the polycyclization mechanisms of **8**. Time-dependent inactivation by **7** and **8** would have occurred due to the covalent-bond formation of this cyclase with intermediary cations **29** and **30–34**, respectively, as discussed in the enzymatic reaction of **6** with hog-liver cyclase.<sup>[11]</sup>

## Conclusion

In conjunction with previously published results,<sup>[9–13]</sup> we conclude that the Me-29 group of **1** is critical to the correct folding of the substrate in the enzyme cavity, with lesser contributions from the other branched methyl groups, such as Me-26, Me-27, and Me-28. Although lanosterol synthase folds **1** in a normal chair-boat-chair-chair conformation, the nor-substrate **8** was folded in two different conformations. The unusual chair-chair-boat-chair conformation afforded the 6,6,6,6-fused tetracyclic skeleton **15**, whereas the normal chair-boat-chair-chair conformation gave the 6,6,6,6-fused tetracycle **14**. Products **14** and **15** were diastereomers that have opposite stereochemistry at C-13 and C-14. This report is the first to describe the importance of the Me-29 group for the correct folding of **1** and the generation of the new triterpene scaffold by using hog-liver cyclase. Furthermore, this study highlights the reason why a five-membered D ring is constructed during lanosterol biosynthesis instead of a six-membered ring.

## Experimental Section

**General analytical methods:** NMR spectra of the enzymic products were recorded in CDCl<sub>3</sub> on Bruker DMX 600 and DPX 400 spectrometers, the chemical shifts are given in ppm relative to the solvent peak  $\delta_{\text{H}}=7.26$  and  $\delta_{\text{C}}=77.0$  ppm as the internal reference for the <sup>1</sup>H and <sup>13</sup>C NMR spectra, respectively. The chemical shifts are given in ppm relative to the solvent peak in C<sub>6</sub>D<sub>6</sub> ( $\delta_{\text{H}}=7.28$  and  $\delta_{\text{C}}=128.0$  ppm). The chemical shifts of the solvent peaks were assigned to be  $\delta_{\text{H}}=2.04$  and  $\delta_{\text{C}}=29.8$  ppm in (CD<sub>3</sub>)<sub>2</sub>CO. The coupling constants *J* are given in Hz. GC analyses were recorded on a Shimadzu GC-8A chromatograph equipped with a flame-ionization detector (a DB-1 capillary column; 30 m × 0.25 mm × 0.25  $\mu\text{m}$ ; J&W Scientific Inc.). GC-MS spectra were recorded on a JEOL SX 100 or a JEOL JMS-Q1000 GC K9 instrument equipped with a ZB-5 ms capillary column (30 m × 0.25 mm × 0.25  $\mu\text{m}$ ; Zebron) by using the EI mode operated at 70 eV. HRMS (EI) was performed by using a direct-inlet system. HPLC was carried out with Hitachi L-1700 (pump) and L-7405 (UV detector), and the HPLC peaks were monitored at  $\lambda=210$  or 214 nm. Specific rotation values were measured with a Horiba SEPA-300 polarimeter.

**Syntheses of noroxidosqualenes **5**, **7** and **8**:** All the synthetic experiments were carried out in a N<sub>2</sub> atmosphere. The syntheses of **5**, **7**, and **8** were performed by using essentially identical methods and with the same reagents. The detailed synthetic processes are described in the Supporting Information (see Figures S1–S4).

**Preparation of ethyl-substituted oxidosqualene **9** (see Figure S4 in the Supporting Information):** Triphenylphosphine (17 g, 64.8 mmol) and ethyl 2-bromobutyrate **48** (10 g, 51.3 mmol) were heated to reflux for 12 h in toluene to give phosphorane **49**. The Wittig reaction of (4*E*,8*E*,12*E*)-4,9,13,17-tetramethyloctadeca-4,8,12,16-tetraenal (**18**) with **49** gave (2*E*,6*E*,10*E*,14*E*)-ethyl-2-ethyl-6,11,15,19-tetramethylcosa-2,6,10,14,18-pentaenoate (**50**; 84%), 1.05 g (2.53 mmol) of which was subjected to reduction with DIBAL-H (hexane solution, 0.98 mol L<sup>-1</sup>, 5.93 mL (5.81 mmol)) to yield alcohol **51** (96%). Next, **51** was transformed into the bromohydrin derivative **52**, which was then converted into the corresponding bromide **54**. The phenylsulfone derivative **41**, prepared from 3-methylbut-2-en-1-ol (**39**), and **54** were coupled with *n*BuLi to afford C<sub>31</sub>-phenylsulfone **55**, followed by reduction with super hydride to yield **9**.

**Preparation of hog-liver cyclase (lanosterol synthase) and the incubation conditions of 2,3-oxidosqualene and its analogues:** Hog liver (100 g) was homogenized at 4 °C in a Waring blender with tris(hydroxymethyl)amino-

methane hydrochloride (Tris-HCl) buffer (90 mL, 0.1 M, pH 7.4) containing ethylenediaminetetraacetic acid (EDTA; 1 mM), phenylmethylsulfonyl fluoride (40  $\mu\text{g mL}^{-1}$ ), and mercaptoethanol (1 mM). The reaction mixture was centrifuged for 10 min at  $17000\times g$  at 4°C. The supernatant was further centrifuged at  $100000\times g$  for 90 min. The resulting microsomal pellets were resuspended and homogenized in the original quantity of Tris-HCl buffer containing EDTA (1 mM), mercaptoethanol (1 mM), and 0.5% Triton X-100 by using a Potter-Elvehjem homogenizer and was centrifuged at  $100000\times g$  for 90 min. The supernatant was used as the enzyme source with a typical protein content of 20–25  $\text{mg mL}^{-1}$ . Substrate **1** and its analogues **5**, **7**, **8**, and **9** (200  $\mu\text{g}$ ) were emulsified with Triton X-100 (2.8 mg) in Tris-HCl buffer (0.1 M, 0.2 mL, pH 7.4). The solution was flushed with nitrogen and incubated for 12 h at 37°C under anaerobic conditions. KOH in methanol (15%, 4 mL) was added to the mixture to terminate the reaction. The incubation tube was heated to 70°C for 30 min to saponify the reaction mixture before extraction with hexane (3  $\times$  1 mL). The organic layer was evaporated under reduced pressure to give a residue, which was dissolved in hexane/EtOAc (10:2) and applied to a short column of  $\text{SiO}_2$  gel to remove the excess Triton X-100. Analysis with GC (Shimadzu, GC-8 A chromatograph) equipped with a DB-1 capillary column (0.53 mm  $\times$  30 m) was used to examine the product profiles (injection temperature = 290°C, column temperature = 280°C, carrier gas = 0.75  $\text{kg cm}^{-2}$ ). Large-scale incubations were conducted to isolate the enzymatic products.

**Isolation of enzymic products 12 and 13 from 7, 14 and 15 from 8, and 16 from 9:**

Chemically synthesized ( $\pm$ )-**7** (60 mg; see Figure S2 in the Supporting Information) was anaerobically incubated with the microsomal protein from pig liver for 12 h at 37°C. The enzymatic reactions were terminated by adding KOH in methanol (15%) and heating to 70°C for 30 min. The enzymatic products of **7** were extracted with hexane and purified by column chromatography on  $\text{SiO}_2$  gel, followed by normal-phase HPLC with hexane/2-PrOH (100:0.05) as the eluent to afford the pure product **12** (4.0 mg). The fraction containing **13** was contaminated with other substances, therefore the entire fraction was acetylated with  $\text{Ac}_2\text{O}$ /pyridine, and pure **13**-acetate (0.4 mg) was separated by HPLC with hexane/2-PrOH (100:0.05) as the eluent.

Anaerobic incubation of the synthesized ( $\pm$ )-**8** (40 mg; see Figure S2 in the Supporting Information) afforded two enzymatic products **14** and **15**. Lipophilic materials were extracted with hexane after saponification. The products were partially purified by column chromatography on  $\text{SiO}_2$  gel, followed by acetylation with  $\text{Ac}_2\text{O}$ /pyridine. The pure acetates of **14** (0.7 mg) and **15** (0.8 mg) were obtained by reversed-phase HPLC ( $\text{C}_{18}$ ; MeOH/ $\text{H}_2\text{O}$  100:4).

Anaerobic incubation of ( $\pm$ )-**9** (6 mg) afforded **16** (1.8 mg) as a single product, which was purified by column chromatography on  $\text{SiO}_2$  gel and HPLC (hexane/THF 100:0.5).

**Spectroscopic data for products 10 and 12–16:**

**Product 10:**  $[\alpha]_{\text{D}}^{20} = +19.08$  ( $c = 0.23$  in  $\text{CHCl}_3$ );  $^1\text{H NMR}$  (400 MHz,  $\text{C}_6\text{D}_6$ ):  $\delta = 0.960$  (s, 3H; Me-28), 1.024 (s, 3H; Me-29), 1.093 (s, 3H; Me-18), 1.094 (d, 3H,  $J = 6.4$  Hz; Me-20), 1.159 (s, 3H; Me-27), 1.23 (m, 2H; H-12), 1.24 (m; H-1), 1.32 (m; H-21), 1.47 (m; H-15), 1.53 (m; H-16), 1.58 (m; H-15), 1.59 (m, 3H; H-2, H-6), 1.60 (m; H-13), 1.63 (m; H-21), 1.66 (m; H-19), 1.70 (m; H-1), 1.719 (s, 3H; Me-25), 1.76 (m; H-17), 1.77 (m; H-6), 1.821 (s, 3H; Me-26), 1.95 (m; H-16), 2.12 (m; H-11), 2.14 (m; H-22), 2.22 (m; H-11), 2.27 (m, 3H; H-7, H-22), 3.17 (dd,  $J = 9.2, 7.2$  Hz; H-3), 5.36 ppm (t,  $J = 6.8$  Hz; H-23);  $^{13}\text{C NMR}$  (100 MHz,  $\text{C}_6\text{D}_6$ ):  $\delta = 15.73$  (q; C-28), 17.72 (q; C-26), 18.60 (q; C-20), 18.80 (t; C-6), 20.35 (q; C-18, C-29)), 22.78 (t; C-12), 23.87 (t; C-11), 25.87 (q; C-25), 26.11 (t; C-16), 26.73 (t; C-22), 26.94 (t; C-7), 28.25 (q; C-27), 28.44 (t; C-2), 34.06 (t; C-21), 35.63 (d; C-19), 35.88 (t; C-15), 36.24 (t; C-1), 37.38 (s; C-10), 39.15 (s; C-4), 45.61 (s; C-14), 45.74 (d; C-17), 48.02 (d; C-13), 50.89 (d; C-5), 78.44 (d; C-3), 125.6 (d; C-23), 130.9 (s; C-25), 136.2 (s; C-9), 136.9 ppm (s; C-8); MS (EI):  $m/z$  (%): 69 (42), 95 (18), 109 (18), 135 (16), 175 (16), 379 (68), 397 (100), 412 (50) [ $M^+$ ]; HRMS (EI): calcd for  $\text{C}_{29}\text{H}_{48}\text{O}$ : 412.3705; found: 412.3703.

**Product 12:**  $[\alpha]_{\text{D}}^{20} = +22.9$  ( $c = 0.2$  in  $\text{CHCl}_3$ );  $^1\text{H NMR}$  (600 MHz,  $\text{CHCl}_3$ ):  $\delta = 0.590$  (s, 3H; Me-18), 0.810 (s, 3H; Me-29), 0.937 (d, 3H,  $J =$

6.5 Hz; H-21), 0.984 (s, 3H; Me-19), 0.996 (s, 3H; Me-28), 1.02 (m, 2H; H-22), 1.13 (bd,  $J = 12.8$  Hz; H-5), 1.14 (m; H-17), 1.26 (m; H-1), 1.28 (m; H-15), 1.30 (m; H-16), 1.37 (m, 1H; H-20), 1.38 (m; H-12), 1.50 (m; H-6), 1.58 (m, 2H; H-2, H-16), 1.600 (s, 3H; Me-27), 1.68 (m; H-6), 1.6801 (s, 3H; Me-26), 1.69 (m; H-2), 1.74 (m; H-1), 1.82 (m; H-23), 1.84 (m; H-15), 1.90 (m; H-7), 1.98 (m, 2H; H-12, H-23)), 2.02 (m, 1H; H-14), 2.04 (m; H-7), 2.06 (m, 2H; H-11), 3.24 (dd,  $J = 10.9, 3.3$  Hz; H-3), 5.09 ppm (t,  $J = 6.9$  Hz; H-24);  $^{13}\text{C NMR}$  (150 MHz,  $\text{CDCl}_3$ ):  $\delta = 11.25$  (q; C-18), 15.35 (q; C-29), 17.62 (q; C-27), 18.44 (t; C-6), 18.63 (q; C-21), 19.84 (q; C-19), 22.05 (t; C-11), 23.78 (t; C-16), 24.80 (t; C-23), 25.71 (q; C-26), 27.91 (t; C-2), 27.95 (q; C-28), 28.45 (t; C-7), 28.79 (t; C-15), 35.76 (t; C-1), 36.04 (t; C-22), 36.07 (d; C-20), 36.98 (t; C-12), 38.93 (s, 2C, C-4, C-10), 42.12 (s; C-13), 50.24 (d; C-5), 51.89 (d; C-14), 54.79 (d; C-17), 78.97 (d; C-3), 125.2 (d; C-24), 128.0 (s; C-8), 130.9 (s; C-25), 135.9 ppm (s; C-9); MS (EI):  $m/z$  (%): 69 (84), 135 (50), 241 (12), 245 (16), 259 (22), 397 (35), 412 (100) [ $M^+$ ]; HRMS (EI): calcd for  $\text{C}_{29}\text{H}_{48}\text{O}$ : 412.3705; found: 412.3715.

**Product 13-acetate:**  $[\alpha]_{\text{D}}^{20} = -9.375$  ( $c = 0.04$  in  $\text{CHCl}_3$ );  $^1\text{H NMR}$  (600 MHz,  $\text{C}_6\text{D}_6$ ):  $\delta = 0.843$  (s, 3H; Me-25), 0.85 (m; H-5), 0.92 (m; H-9), 0.94 (m; H-12), 1.016 (s, 3H; Me-23), 1.049 (s, 3H; Me-24), 1.13 (m; H-1), 1.30 (m; H-11), 1.33 (m; H-6), 1.40 (m; H-8), 1.45 (m; H-1), 1.46 (m; H-11), 1.62 (m; H-7), 1.63 (m; H-6), 1.673 (s, 3H; Me-29), 1.728 (s, 3H; Me-26), 1.74 (m; H-2), 1.773 (s, 3H; Me-27), 1.801 (s, 3H; Me-28), 1.873 (s, 3H; acetyl Me), 1.88 (m; H-2), 1.91 (m; H-7), 169.8 (s, COO), 2.08 (m; H-13), 2.11 (m; H-12), 2.23 (bt, 2H,  $J = 7.0$  Hz; H-19), 2.29 (m, 2H; H-20), 3.00 (t,  $J = 6.7$  Hz; H-16), 4.85 (dd,  $J = 12.5, 4.5$  Hz; H-3), 5.36 (bt,  $J = 6.8$  Hz; H-21), 5.53 (bt,  $J = 6.8$  Hz; H-17), 5.56 ppm (bt,  $J = 6.8$  Hz; H-15);  $^{13}\text{C NMR}$  (150 MHz,  $\text{C}_6\text{D}_6$ ):  $\delta = 13.35$  (q; C-26), 13.59 (q; C-25), 17.72 (q; C-29), 16.16 (q; C-27), 16.79 (q; C-24), 20.84 (q, acetyl Me), 21.83 (t; C-6), 22.92 (t; C-11), 25.82 (q; C-28), 27.14 (t; C-20), 27.44 (t; C-16), 28.36 (q; C-23), 29.01 (t; C-12), 24.33 (t; C-2), 31.52 (t; C-7), 36.38 (s; C-10), 37.42 (t; C-1), 37.88 (s; C-4), 40.15 (t; C-19), 42.44 (d; C-8), 54.99 (d; C-5), 55.22 (d; C-13), 59.14 (d; C-9), 83.00 (d; C-3), 123.6 (d; C-17), 124.0 (d; C-15), 124.9 (d; C-21), 131.1 (s; C-22), 134.9 (s; C-18), 136.4 (s; C-14), 169.8 ppm (s, acetyl CO); MS (EI):  $m/z$  (%): 69 (97), 161 (52), 109 (68), 123 (100), 135 (63), 177 (33), 215 (35), 329 (32), 454 (23) [ $M^+$ ]; HRMS (EI): calcd for  $\text{C}_{31}\text{H}_{50}\text{O}_2$ : 454.3811; found: 454.3820.

**Product 14-acetate:**  $[\alpha]_{\text{D}}^{20} = -29.32$  ( $c = 0.054$  in  $\text{CHCl}_3$ );  $^1\text{H NMR}$  (600 MHz,  $\text{CDCl}_3$ ):  $\delta = 0.687$  (s, 3H; Me-19), 0.83 (m; H-21), 0.876 (s, 6H; Me-27, Me-28), 0.983 (s, 3H; Me-29), 0.990 (s, 3H, Me-20), 1.12 (m; H-12), 1.13 (bd,  $J = 12.8$  Hz; H-5), 1.31 (m; H-1), 1.32 (m; H-15), 1.38 (m; H-18), 1.42 (m, 2H; H-12, H-15), 1.46 (m; H-6), 1.50 (m; H-21), 1.53 (m, 2H; H-16), 1.56 (m; H-12), 1.599 (s, 3H; Me-26), 1.62 (m, 2H; H-2, H-12), 1.68 (m; H-6), 1.686 (s, 3H; Me-25), 1.70 (m; H-2), 1.76 (m; H-1), 1.80 (m; H-22), 1.95 (m; H-7), 1.98 (m; H-11), 2.03 (m; H-11), 2.04 (m; H-22), 2.050 (s, 3H; acetyl Me), 2.10 (m; H-7), 4.50 (dd,  $J = 11.8, 4.5$  Hz; H-3), 5.10 ppm (t,  $J = 7.0$  Hz; H-23);  $^{13}\text{C NMR}$  (150 MHz,  $\text{CDCl}_3$ ):  $\delta = 14.22$  (q; C-19), 16.50 (q; C-28), 17.66 (q; C-26), 18.46 (t; C-6), 19.28 (q; C-20), 19.62 (t; C-11), 21.32 (q, acetyl Me), 21.44 (t; C-16), 22.01 (q; C-29), 24.23 (t; C-2), 25.71 (q; C-25), 25.71 (t; C-7), 26.67 (t; C-17), 26.99 (t; C-22), 27.87 (q; C-27), 29.15 (t; C-12), 30.47 (t; C-21), 30.52 (t; C-15), 35.37 (t; C-1), 37.15 (s; C-14), 37.27 (s; C-10), 37.76 (s; C-4), 40.34 (s; C-13), 40.43 (d; C-18), 49.98 (d; C-5), 80.96 (d; C-3), 125.3 (d; C-23), 131.0 (s; C-24), 134.3 (s; C-9), 135.2 (s; C-8), 170.8 ppm (s, acetyl CO); the following  $^{13}\text{C NMR}$  signals are indistinguishable from each other because they have very similar chemical shifts: C-10/C-14, C-15/C-21; MS (EI):  $m/z$  (%): 69 (100), 229 (92), 241 (54), 289 (43), 301 (32), 379 (39), 379 (38), 439 (63), 454 (73) [ $M^+$ ]; HRMS (EI): calcd for  $\text{C}_{31}\text{H}_{50}\text{O}_2$ : 454.3811; found: 454.3805; assignments of the  $^1\text{H}$  and  $^{13}\text{C NMR}$  data in  $[\text{D}_6]$ acetone are shown in the Supporting Information.

**Product 15-acetate:**  $[\alpha]_{\text{D}}^{20} = 67.98$  ( $c = 0.038$  in  $\text{CHCl}_3$ );  $^1\text{H NMR}$  (600 MHz,  $\text{CDCl}_3$ ):  $\delta = 0.872$  (s, 6H; Me-27, Me-28), 0.908 (s, 3H; Me-19), 0.95 (m; H-12), 0.978 (s, 3H; Me-29), 0.991 (s, 3H; Me-20), 1.11 (dd,  $J = 12.6, 2.1$  Hz; H-5), 1.15 (m, 1H; H-18), 1.26 (m; H-21), 1.27 (m; H-15), 1.33 (m; H-1), 1.42 (m; H-17), 1.44 (m; H-16), 1.46 (m; H-6), 1.55 (m; H-15), 1.56 (m; H-16), 1.592 (s, 3H; Me-26), 1.62 (m, 2H; H-2, H-21), 1.65 (m; H-6), 1.683 (s, 3H; Me-25), 1.71 (m; H-2), 1.75 (m; H-22), 1.76 (m; H-1), 1.81 (m; H-17), 1.95 (m; H-7), 2.00 (m, 2H; H-11, H-22),

2.048 (s, 3H; acetyl Me), 2.07 (m; H-7), 2.08 (m, 2H; H-11, H-12), 4.50 (dd,  $J=11.8$ , 4.4 Hz; H-3), 5.10 ppm (t,  $J=7.0$  Hz; H-23);  $^{13}\text{C}$  NMR (150 MHz,  $\text{CDCl}_3$ ):  $\delta=16.49$  (q; C-28), 17.67 (q; C-26), 18.19 (t; C-6), 18.31 (t; C-16), 19.29 (q; C-20), 20.14 (t; C-11), 21.32 (q, acetyl Me), 23.15 (q; C-19), 23.79 (q; C-29), 24.24 (t; C-2), 24.40 (t; C-17), 24.65 (t; C-7), 25.71 (q; C-25), 27.87 (q; C-27), 29.28 (t; C-12), 29.37 (t; C-22), 29.92 (t; C-21), 31.01 (t; C-15), 35.55 (t; C-1), 37.18 (s; C-14), 37.24 (s; C-10), 37.77 (s; C-4), 39.54 (s; C-13), 45.24 (d; C-18), 49.96 (d; C-5), 80.93 (d; C-3), 125.1 (d; C-23), 131.2 (s; C-24), 133.9 (s; C-9), 136.1 (s; C-8), 171.0 ppm (s, acetyl CO); the following  $^{13}\text{C}$  NMR signals are indistinguishable from each other because they have very similar chemical shifts: C-10/C-14, C-12/C-22, C-6/C-16; MS (EI):  $m/z$  (%): 69 (100), 229 (84), 241 (48), 289 (28), 301 (23), 379 (39), 379 (25), 439 (36), 454 (68) [ $M^+$ ]; HRMS (EI): calcd for  $\text{C}_{31}\text{H}_{50}\text{O}_2$ : 454.3811; found: 454.3817; assignments of the  $^1\text{H}$  and  $^{13}\text{C}$  NMR data in  $\text{C}_6\text{D}_6$  are shown in Figure S9 in the Supporting Information.

**Product 16:**  $[\alpha]_D^{20}=18.62$  ( $c=0.188$  in  $\text{CHCl}_3$ );  $^1\text{H}$  NMR (400 MHz,  $\text{CDCl}_3$ ):  $\delta=0.687$  (s, 3H; Me-18), 0.795 (t,  $J=7.2$  Hz; Me-31), 0.808 (3H; s, Me-29), 0.882 (s, 3H; Me-30), 0.978 (s, 3H; Me-19), 0.998 (s, 3H; Me-28), 1.16 (m; H-15), 1.20 (m; H-22), 1.22 (m; H-1), 1.36 (m; H-22), 1.37 (m; H-20), 1.38 (m; H-21), 1.50 (m; H-6), 1.53 (m, 2H; H-16, H-21), 1.56 (m; H-2), 1.58 (m; H-15), 1.581 (brd,  $J=11.8$ , 2.0 Hz; H-5), 1.605 (s, 3H; Me-27), 1.63 (m; H-2), 1.64 (m; H-12), 1.67 (m; H-6), 1.682 (s, 3H; Me-26), 1.71 (m; H-17), 1.73 (m; H-1), 1.77 (m; H-12), 1.82 (m; H-23), 1.97 (brm, 2H; H-23), 2.01  $\alpha$ (m, 2H; H-11), 2.03 (m, 2H; H-7), 2.07 (m; H-16), 3.23 (dd,  $J=11.6$ , 4.4 Hz; H-3), 5.11 ppm (t,  $J=6.8$  Hz; H-24);  $^{13}\text{C}$  NMR (100 MHz,  $\text{CDCl}_3$ ):  $\delta=9.15$  (q; C-31), 15.42 (q; C-29), 15.67 (q; C-18), 17.62 (q; C-27), 18.26 (t; C-6), 19.15 (q; C-19), 21.05 (t; C-11), 22.53 (t; C-21), 24.35 (t; C-23), 24.43 (q; C-30), 25.74 (q; C-26), 26.49 (t; C-7), 27.85 (t; C-16), 27.93 (t; C-2), 27.96 (q; C-28), 30.64 (t; C-22), 30.69 (t; C-12), 30.79 (t; C-15), 35.60 (t; C-1), 37.01 (s; C-10), 38.89 (s; C-4), 40.86 (d; C-20), 44.46 (s; C-13), 45.95 (d; C-17), 49.87 (s; C-14), 50.38 (d; C-5), 78.98 (d; C-3), 125.3 (d; C-24), 130.8 (s; C-25), 134.3 (s; C-9), 134.4 ppm (s; C-8); the following  $^{13}\text{C}$  NMR signals are indistinguishable from each other because they have very similar chemical shifts: C-2/C-16, C-15/C-22; MS (EI):  $m/z$  (%): 69 (100), 81 (32), 95 (46), 123 (30), 407 (47), 425 (82), 440 (33) [ $M^+$ ]; HRMS (EI): calcd for  $\text{C}_{31}\text{H}_{52}\text{O}$ : 440.4018; found: 440.4018.

**Kinetic analyses  $k_{\text{inact}}$  and  $K_i$  of time-dependent inhibition by 5, 7, and 8:** The partially purified lanosterol synthase described above (1.8 mL) was used. Noroxidosqualenes 5, 7, and 8 were added to the enzyme solution, which was adjusted to a final volume of 2.0 mL with Tris-HCl buffer (0.1 M, pH 7.4): 30  $\mu\text{M}$ , 60  $\mu\text{M}$ , and 121  $\mu\text{M}$  for 5 and 8; 60  $\mu\text{M}$ , 121  $\mu\text{M}$ , and 242  $\mu\text{M}$  for 7. Each of the solutions was incubated at 37°C for the intervals of 0, 30, 60, 120, and 300 min. From each of the reaction tubes, an aliquot of the preincubated mixture (200  $\mu\text{L}$ ) was added to a tube containing ( $\pm$ )-1 (200  $\mu\text{g}$ ) and then further incubation was conducted for 8 h. To quench the reaction, KOH in MeOH (15%, 1 mL) was added and the solution was heated at 80°C for 30 min. The hexane extract was subjected to GC analysis to estimate the amount of lanosterol produced. The kinetic parameters of  $k_{\text{inact}}$  and  $K_i$  were determined using Kitz-Wilson plots. Ethyl-substituted 9 did not undergo any time-dependent inhibition.

## Acknowledgements

This work was supported in part by Grant-in-Aid for Scientific Research from the Ministry of Education, Culture, Sports, Science and Technology (Japan).

- [1] Reviews for the polycyclization of triterpene cyclases: a) T. Hoshino, T. Sato, *Chem. Commun.* **2002**, 291–301; b) K. U. Wendt, G. E. Schulz, E. J. Corey, D. R. Liu, *Angew. Chem.* **2000**, *112*, 2930–2952; *Angew. Chem. Int. Ed.* **2000**, *39*, 2812–2833; c) G. Siedenburg, D. Jendrossek, *Appl. Environ. Microbiol.* **2011**, *77*, 3905–3915; d) R. A. Yoder, J. N. Johnston, *Chem. Rev.* **2005**, *105*, 4730–4756; e) R. Xu, G. C. Fazio, S. P. T. Matsuda, *Phytochemistry* **2004**, *65*, 261–291; f) T.-K. Wu, C.-H. Chang, Y.-T. Liu, T.-T. Wang, *Chem. Rec.* **2008**, *8*, 302–305; g) I. Abe, *Nat. Prod. Rep.* **2007**, *24*, 1311–1331.
- [2] A. Eschenmoser, L. Ruzicka, O. Jeger, D. Arigoni, *Helv. Chim. Acta* **1955**, *38*, 1890–1940.
- [3] J. W. Cornforth, *Angew. Chem. Int. Ed. Engl.* **1968**, *7*, 903–911.
- [4] E. J. Corey, S. C. Virgil, *J. Am. Chem. Soc.* **1991**, *113*, 4025–4026.
- [5] E. J. Corey, S. C. Virgil, S. Sarshar, *J. Am. Chem. Soc.* **1991**, *113*, 8171–8172.
- [6] A. Eschenmoser, D. Arigoni, *Helv. Chim. Acta* **2005**, *88*, 3011–3050.
- [7] J.-L. Giner, S. Rocchetti, S. Neunlist, M. Rohmer, D. Arigoni, *Chem. Commun.* **2005**, 3089–3091.
- [8] I. Abe, M. Rohmer, G. D. Prestwich, *Chem. Rev.* **1993**, *93*, 2189–2206.
- [9] E. J. Corey, A. Krief, H. Yamamoto, *J. Am. Chem. Soc.* **1971**, *93*, 1493–1494.
- [10] E. E. van Tamelen, R. P. Hanzlik, K. B. Sharpless, R. B. Clayton, W. J. Richter, *J. Am. Chem. Soc.* **1968**, *90*, 3284–3286.
- [11] E. J. Corey, S. C. Virgil, D. R. Liu, S. Sarshar, *J. Am. Chem. Soc.* **1992**, *114*, 1524–1525.
- [12] R. B. Clayton, E. E. van Tamelen, R. G. Nadeau, *J. Am. Chem. Soc.* **1968**, *90*, 820–821.
- [13] E. J. Corey, K. Lin, M. Jautelat, *J. Am. Chem. Soc.* **1968**, *90*, 2724–2726.
- [14] A. G. Byskov, C. Y. Andersen, L. Leonardsen, M. Baltsen, *J. Exp. Zool. Part B* **1999**, *285*, 237–242.
- [15] T. Hoshino, E. Ishibashi, K. Kaneko, *J. Chem. Soc. Chem. Commun.* **1995**, 2401–2402.
- [16] T. Hoshino, Y. Sakai, *Tetrahedron Lett.* **2001**, *42*, 7319–7323.
- [17] T. Hoshino, Y. Sakai, *Chem. Commun.* **1998**, 1591–1592.
- [18] R. Thoma, T. Schulz-Gasch, B. D'Arcy, J. Benz, J. Aebi, H. Dehmlo, M. Hennig, M. Stihle, A. Ruf, *Nature* **2004**, *432*, 118–122.
- [19] T.-K. Wu, C.-H. Chang, H.-Y. Wen, Y.-T. Liu, W.-H. Li, T.-T. Wang, W.-S. Shie, *Org. Lett.* **2010**, *12*, 500–503.
- [20] T.-K. Wu, Y.-C. Chang, Y.-T. Liu, C.-H. Chang, H.-Y. Wen, W.-H. Li, W.-S. Shi, *Org. Biomol. Chem.* **2011**, *9*, 1092–1097.
- [21] T.-K. Wu, T.-T. Wang, C.-H. Chang, Y.-T. Liu, W.-S. Shi, *Org. Lett.* **2008**, *10*, 4959–4962.
- [22] T. Hoshino, M. Kouda, T. Abe, S. Ohashi, *Biosci. Biotechnol. Biochem.* **1999**, *63*, 2038–2041.
- [23] N. Morikubo, Y. Fukuda, K. Ohtake, N. Shinya, D. Kiga, K. Sakamoto, M. Asanuma, H. Hirota, S. Yokoyama, T. Hoshino, *J. Am. Chem. Soc.* **2006**, *128*, 13184–13194.

Received: May 21, 2012

Revised: June 26, 2012

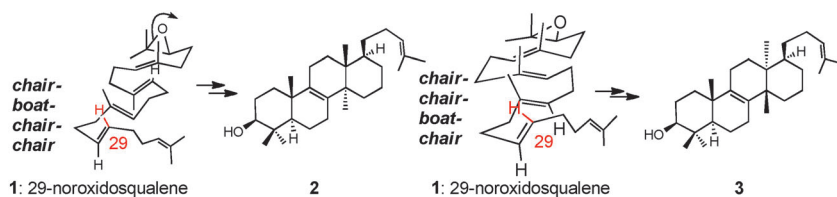
Published online: ■ ■ ■, 0000

**Enzyme Catalysis**

T. Hoshino,\* A. Chiba,  
N. Abe .....



**Lanosterol Biosynthesis: The Critical Role of the Methyl-29 Group of 2,3-Oxidosqualene for the Correct Folding of this Substrate and for the Construction of the Five-Membered D Ring**



**Ringing in the changes:** The incubation of **1** with porcine-liver cyclase afforded new nortriterpenes **2** and **3** with 6,6,6,6-fused tetracyclic skeletons, which were produced by chair-boat-chair-chair and chair-chair-boat-chair

conformations, respectively (see scheme), thus indicating that the 29-methyl group is critical to the correct folding of oxidosqualene and to the formation of the five-membered D ring for lanosterol biosynthesis.